JOURNAL OF THE KOREAN ASTRONOMICAL SOCIETY
37: 243 ~ 248, 2004

FORMATION OF INTERMEDIATE-SCALE STRUCTURES IN SPIRAL GALAXIES

WOONG-TAE KIM
Astronomy Program, SEES, Seoul National University, Seoul 151-742, Korea
E-mail: wkim@astro.snu.ac.kr
(Received July 21, 2004; Accepted December 10, 2004)

ABSTRACT

Disk galaxies abound with intermediate-scale structures such as OB star complexes, giant clouds, and dust spurs in a close geometrical association with spiral arms. Various mechanisms have been proposed as candidates for their origin, but a comprehensive theory should encompass fundamental physical agents such as self-gravity, magnetic fields, galactic differential rotation, and spiral arms, all of which are known to exist in disk galaxies. Recent numerical simulations incorporating all these physical processes show that magneto-Jeans instability (MJI), in which magnetic tension resists the stabilizing Coriolis force of galaxy rotation, is much more powerful than swing-amplification or the Parker instability in forming self-gravitating intermediate-scale structures. The MJI occurring in shearing and expanding flows off spiral arms rapidly forms structures elongated along the direction perpendicular to the arms, remarkably similar to dust spurs seen in *HST* images of spiral galaxies. In highly nonlinear stages, these spurs fragment to form bound clumps, possibly evolving into bright arm and interarm H II regions, suggesting that all these intermediate-scale structures in spiral galaxies probably share a common dynamical origin.

Key words : galaxies: ISM — galaxies: structure — instabilities — ISM: kinematics and dynamics — ISM: magnetic fields — MHD

I. INTRODUCTION

On large scales, disk galaxies display global spiral patterns that wind out over ~ 10 kpc in radius from the central part to almost the outer edge of an optical disk, sharply outlined by bright young star complexes and dark dust lanes. Such large-scale spiral patterns are the manifestation of spiral density waves which propagate with a constant pattern speed through differentially-rotating galactic disks (Lin & Shu 1964, 1966). As the gaseous medium passes through the regions of the potential well of stars, it is easily compressed and shocked to appear as the dark dust lanes. Active star formation is triggered in the compressed dense clouds, resulting in OB star complexes and giant H II regions distributed in a "beads on a string" pattern along the arms (Baade 1963). These OB star complexes and giant H II regions are examples of intermediate-scale (~ 1 kpc) structures or spiral arm substructures. In radios wavelengths, intermediate-scale structures appears as giant molecular associations (Vogel, Kulkarni, & Scoville 1988) or H I superclouds (Elmegreen 1995) with each mass of ~ $10^7 M_\odot$, similar to the characteristic Jeans mass in galactic disks.

Perhaps the most striking intermediate-scale structures are gaseous spurs evident in a recent *HST* image of M51 by Scoville & Rector (2001) that shows dust spurs project almost perpendicularly from the main spiral arms. Like H II regions, spurs are also regularly distributed along the whole length of the arms. These spurs are dotted with H II regions and become trailing in the interarm regions. Although a major portion of H II regions are located along the spiral arms, a significant fraction of them are also found in deep interarm regions (e.g., Scoville et al 2001). Considering the sterile condition of interarm regions where gas surface density is low and shear is strong, the origin of numerous interarm H II regions is puzzling. Do they form at current locations, or are they carried away from spiral arm regions? In any event, strong association of interarm H II regions with gaseous spurs suggest that they may be the products of the common dynamical processes.

One may wonder that dust spurs are unique features of M51 which has strong spiral arms perturbed by a nearby satellite galaxy. But, spurs appear fairly common in many of the Hubble archive images including M74, M100, M109, etc. In particular, La Vigne & Vogel (2003, private communication) examined 258 *HST* galaxies and found that 25 of them exhibit easily-identifiable global spiral arms or bars, of which 19 galaxies contain well-defined dust spurs. This suggests that spiral galaxies with sufficiently strong spiral arms have dust spurs. Since spurs are primarily outlined by narrow dust lanes against a bright background, it may sometimes be difficult to recognize them if they are relatively weak or galaxies are too bright in optical wavebands.

Since the intermediate-scale structures are strongly coupled with ongoing sites of star formation, under-

Proceedings of The 2nd Korea-Mexico Joint Workshop on *Physics of the Diffuse Interstellar Medium*

standing the physical processes that govern their formation is of crucial importance for many related questions in disk galaxies: galactic structure and evolution, global star formation rates, and the nature of the Hubble sequence. In a series of papers (Kim & Ostriker 2001, 2002; Kim, Ostriker, & Stone 2002, 2003), we have studied the formation of intermediate-scale structures via gravitational instability of galactic gaseous disks. Non-linear effect as well as fundamental physical agents such as self-gravity, magnetic fields, galactic differential rotation, and spiral arms have all been incorporated in our models. Here we summarize the main results of this work, with an emphasis on spur formation inside spiral arms. For more detailed results and comprehensive discussions, we refer the interested reader to the original publications cited above.

II. CONDENSATION MECHANISMS

Proposed mechanisms for intermediate-scale structures in disks galaxies include (1) random collisional agglomeration of small clouds, (2) large-scale gravitational instability, and (3) the Parker instability with azimuthal magnetic fields. We review briefly each process in this section.

The first, so-called Oort (1954) model in which highly ballistic, small clouds collide with each other and stick together to grow in size and mass until they become gravitationally unstable has been successful in explaining the observed cloud mass spectrum $dn/dM \propto M^{-\alpha}$ with $\alpha \sim 1.5 - 1.8$ (e.g., Dame et al 1986; Solomon et al 1987). However, the basic premise of the Oort model that a mutual collision of two clouds always leads to a merger turns out to be incorrect, as hydrodynamic simulations for cloud collisions show that the collision outcome is preferentially destruction rather than merger for a supersonic collision (e.g., Lattanzio et al 1995; Kim et al 1999; Klein, Woods, & McKee 2001). Since there is insufficient mass in small clouds to maintain the mass spectrum steady (Blitz & Williams 1999), the collisional build-up model is unlikely to be important in the formation of intermediate-scale structures.

Gravitational instability has been one of the best known condensation processes since Jeans (1902), in which perturbed material with large enough mass collapses under its own weight. An obstacle self-gravity of gas must overcome to collect mass on a large scale in a rotating disk is Coriolis force that produces the stabilizing epicyclic motions. Toomre (1964) showed that a razor-thin, unmagnetized, gaseous disk is completely stable to axisymmetric perturbations provided $Q > 1$ where the Toomre stability parameter

$$Q \equiv \frac{\kappa c_s}{\pi G \Sigma}, \qquad (1)$$

with the epicycle frequency κ, the sound speed c_s, the gravitational constant G, and the surface density Σ of the disk. The finite thickness of disks also plays a stabilizing role by decreasing the critical Q value to $Q_c = 0.678$ for an isothermal disk (Goldreich & Lynden-Bell 1965)*. With the average Q values larger than unity, most disk galaxies would be stable to axisymmetric gravitational instability unless other effects (see below) come into play.

If perturbations are non-axisymmetric, however, self-gravitating condensations can grow even when $Q > 1$ via either swing amplifier or magneto-Jeans instability (MJI). Swing amplification arises when the sense of background shear causes disturbances to sweep in the same direction as epicyclic motions, allowing material to stay longer in wave crests. Consequently, self-gravity is enhanced and perturbations amplify. On the other hand, the MJI relies strictly on the presence of magnetic fields that resist the stabilizing Coriolis force by exerting tension force (Lynden-Bell 1966; Elmegreen 1987). As the magnetic fields extract angular momentum from contracting objects, self-gravity collects more material along the direction parallel to the field lines. In the limit of strong magnetic fields, gravitational instability operates as if disks were non-rotating and unmagnetized, so that the stabilizing effect of rotation is completely removed. This MJI works very efficiently when shear is weak and magnetic fields are strong, as in galactic central parts or inside spiral arms (Kim & Ostriker 2001, 2002) When shear is strong, the kinematic increase of local wavenumbers is so rapid that disturbances are easily stabilized by sound waves.

Parker (1966) demonstrated that driven by magnetic buoyancy, a region of lower (higher) mass-to-flux ratio than the equilibrium state rises up (slides down) along the buckling field lines, reducing (increasing) the mass-to-flux ratio more in the floated (sunk) region and thus expediting the instability. Because of the similarity between the preferred wavelength and growth time of the Parker mode and the mean spacing ($\sim$ 500 pc) and lifetime (a few $\times 10^7$ yr) of giant molecular clouds in the Galactic disks, the Parker instability has been a favored mechanism for giant cloud formation (e.g., Blitz & Shu 1980; Lee, S. M. et al in this volume).

However, the nonlinear consequence of the Parker instability is considered doubtful. Recent numerical studies suggest that the Parker instability *alone* is unable to form clouds in galactic disks (e.g., Kim et al 2000; Santillán et al 2002). The primary reason for this is that Parker instability is not a runaway process but is eventually stabilized by tension forces from bent magnetic field lines. Mouschovias (1974) analytically obtained two-dimensional, final equilibrium states of the Parker instability and showed that column density at magnetic valleys is enhanced only by a factor of 2; corresponding numerical simulations produced similar re-

*Inclusion of an external stellar gravity tends to increase Q_c by compressing the disk vertically. When self-gravity equals external gravity at one scale height of the disk, $Q_c \approx 0.75$ if the disk is unmagnetized (Kim, Ostriker, & Stone 2002).

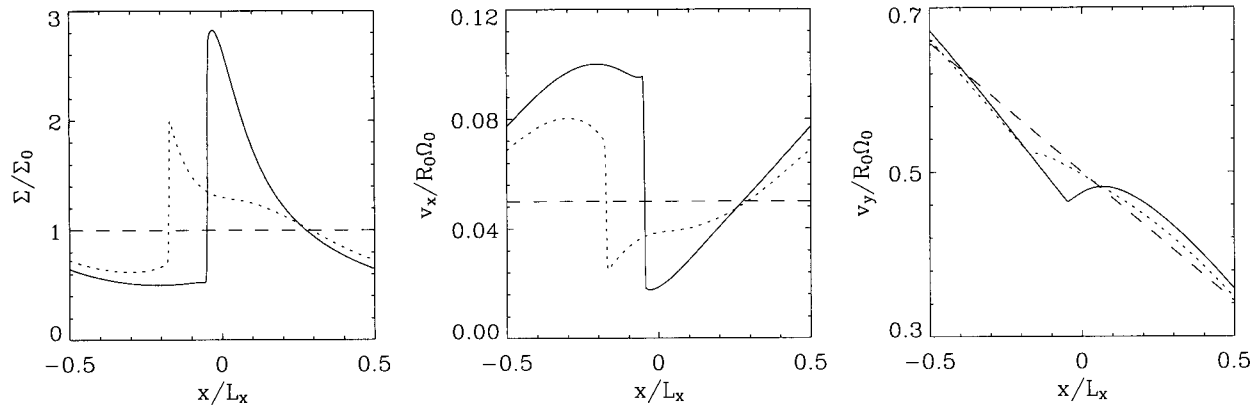

Fig. 1.— Equilibrium spiral shock profiles of (*left*) the gas surface density, (*middle*) x-velocity, (*right*) y-velocity for a model disk with $Q_0 = 1.5$, $F = 3\%$, and thermal equipartition magnetic field strength. In each panel, the solid and dotted curves correspond to the self-gravitating and non-self-gravitating case, respectively, while the dashed curve represents the background state where the stellar potential perturbation is absent. The y-component of magnetic fields follows the surface density distribution closely, indicating that the spiral arm regions also have stronger field strength. Note that shear is reversed (i.e., $dv_y/dx > 0$) in the regions where $\Sigma/\Sigma_0 > 2$, while the other areas have normal shear.

sults (e.g., Kim et al 2000; Santillán et al 2002)†. Moreover, the Parker instability has larger growth rates for smaller-scale perturbations in three dimensions, generating turbulent density and velocity fields rather than well-defined cloud structures (Parker 1967; Lachièze-Rey et al 1980). The level of velocity fluctuations caused by the Parker instability is less than a tenth of sound speed of the medium (Kim, Ostriker, & Stone 2002).

III. SPUR FORMATION INSIDE SPIRAL ARMS

The strong spatial association between intermediate-scale structures and spiral arms suggests that the latter has a direct influence on the formation of the former. By launching shock waves, the presence of stellar spiral potentials can significantly alter the dynamics of a gaseous disk that would otherwise be stable or subject to only mild swing amplification. With high surface density, the shocked material inside spiral arms is more prone to gravitational instability than the cases without spiral arms.

An indispensable ingredient involved in the dynamics of disk galaxies is rotational shear. The shearing time in disks under the solar neighborhood condition is $t_{\rm sh} = -d\ln R/d\Omega \approx 4\times10^7\,{\rm yr}\,(\Omega/26\,{\rm km\,s^{-1}\,kpc^{-1}})^{-1}$, which is shorter than the sound crossing time $t_{\rm s} = L/c_s = 1.5\times10^8\,{\rm yr}\,(L/1\,{\rm kpc})(c_s/7\,{\rm km\,s^{-1}})^{-1}$ or the gravitational contraction time $t_{\rm g} = c_s/G\Sigma = 1.2\times10^8\,{\rm yr}\,(c_s/7\,{\rm km\,s^{-1}})(\Sigma/13\,M_\odot\,{\rm pc^{-2}})^{-1}$. Shear is not only the basis of swing amplification that produces stronger trailing waves, but it can also shape structures of various scales in galactic planes. Nevertheless, shear has been the last component to be included in local galactic disk simulations due, in part, to the technical challenge of handling boundary conditions associated with a linear shear profile. A Lagrangian remap algorithm introduced by Hawley, Gammie, & Balbus (1995) enables self-consistent treatment of linear shear.

Consider a spiral potential that is rotating at an angular velocity Ω_p about the galactic center. To study the local dynamics of gas flow through the potential, it is convenient to work with a two-dimensional local Cartesian box comoving with the potential, whose center lies at the galactocentric radius R_0. The box is slightly tilted in such a way that its two orthogonal axes correspond respectively to the directions perpendicular (x-axis) and parallel (y-axis) to the local arm segment. In this local spiral coordinate system, the background velocity profile due to galaxy rotation is given by $\mathbf{v}_0 = R_0(\Omega_0-\Omega_p)\sin i\hat{\mathbf{x}} + [R_0(\Omega_0-\Omega_p) - q_0\Omega_0 x]\hat{\mathbf{y}}$, where $\Omega_0 = \Omega(R_0)$, i ($\ll 1$; tightly wound arm) is the pitch angle of the arm relative to the galactocentric circle, and $q_0 = -(d\ln\Omega/d\ln R)|_{R_0}$ measures the shear rate in the background flow in the absence of a spiral arm (Kim & Ostriker 2002). When the box is located away from the corotation radius of the pattern, the x-component of the background velocity is supersonic, resulting in the formation of spiral shocks. If the potential is periodic in x and the medium is isothermal, the shock is one dimensional and steady.

Figure 1 presents an exemplary equilibrium profile of a spiral shock in a disk with $Q_0 = 1.5$ and thermal equipartition magnetic field strength. The nor-

†Although the Parker instability *alone* cannot create gravitationally bound clouds, it may still be important in connection with spiral arms and/or gravitational instability by seeding structures at the Parker scales. See S. M. Lee et al in this volume for detailed discussions of the Parker-Jeans instability.

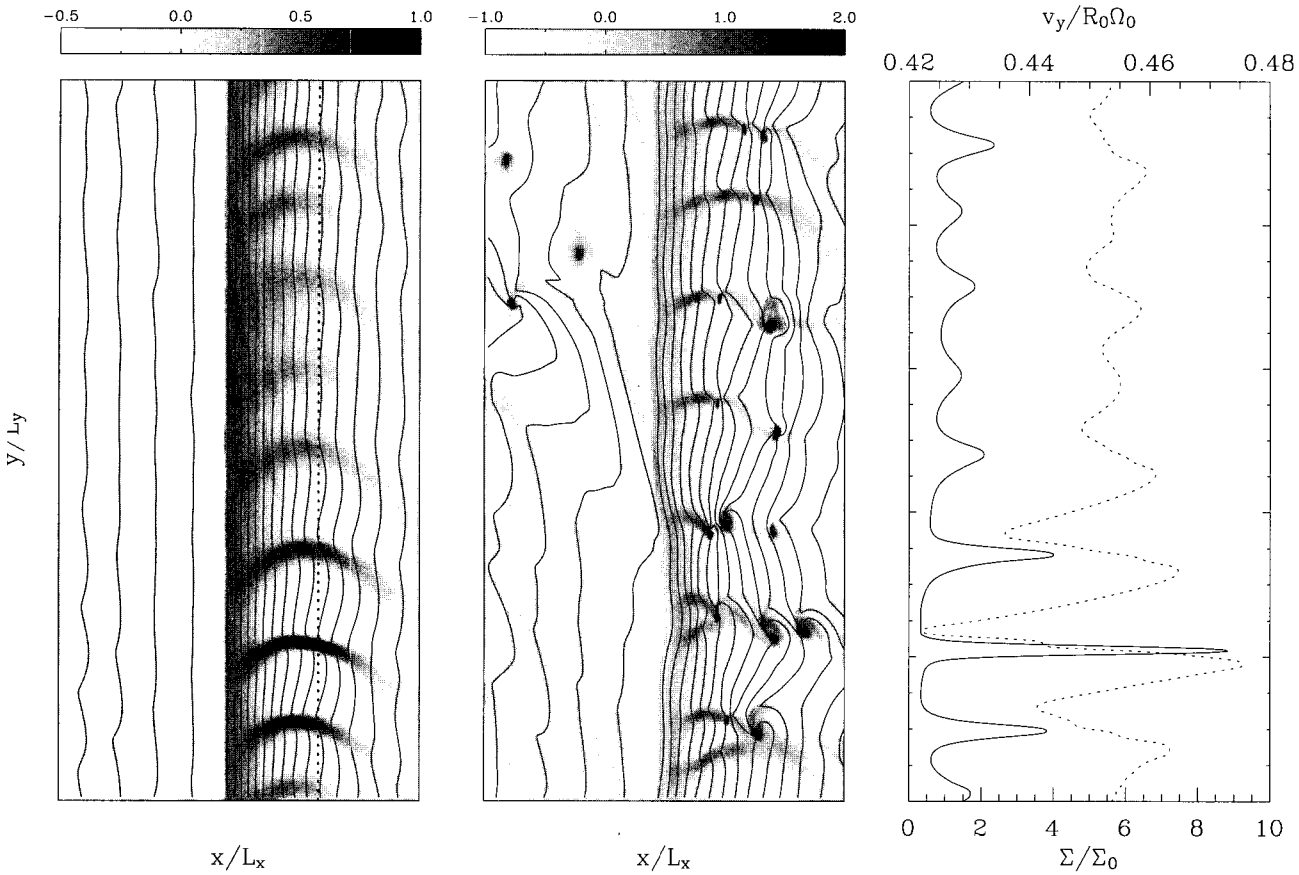

Fig. 2.— Density structures of a two-dimensional MHD simulation with $Q_0 = 1.5$, $F = 3\%$, and thermal equipartition magnetic fields at (*left*) $t = 1.27$ orbits (*middle*) $t = 1.75$ orbits. Grey-scale bars label $\log \Sigma/\Sigma_0$ and solid lines draw magnetic field lines. *Right:* The profiles of surface density (solid line) and y-velocity (dotted line) at $t = 1.27$ orbits along the cut represented by the dotted line in the left panel show that $dv_y/dy < 0$ at the spur locations, indicating that spurs grow by collecting mass mostly along the y-direction.

malized amplitude of the external spiral potential Φ_0 is set to $F \equiv (2/\sin i)|\Phi_0|/(\Omega_0 R_0)^2 = 3\%$; the parameter F measures the perturbed radial force due to the spiral potential relative to the mean axisymmetric gravity. Solid curves in Figure 1 correspond to the self-gravitating case, while dotted curves are for the non-self-gravitating counterpart; the dashed lines draw the unperturbed state. As material flows from left to right, it is readily shocked and compressed. The flow has to move faster after the shock front to meet the imposed periodic boundary conditions. The inclusion of self-gravity moves the shock location downstream and forms a stronger and wider spiral arm. When Q_0 is smaller than a certain value, a stable spiral shock no longer exists because of either gravitational instability or incompatibility of equilibria with a given patten speed. This occurs when $Q_0 < 0.87$ for $F = 3\%$ and equipartition magnetic fields (Kim & Ostriker 2002).

An important aspect of the spiral shocks that is crucial for the formation of intermediate-scale structures is the reduction in the local rotational shear rate. The constraint of the potential vorticity conservation requires $dv_y/dx = \Sigma/\Sigma_0 - 2$, so that shear is reversed ($dv_y/dx > 0$) locally in the spiral arm regions where $\Sigma/\Sigma_0 > 2$. With reversed shear, the kinematic sweeping of disturbances is opposite to the sense of the epicyclic motions, so that it is difficult to expect an efficient operation of swing amplification inside spiral arms. On the other hand, the spatially varying sense of shear keeps the net shear rate close to zero. With enhanced strength of magnetic fields, therefore, the spiral arm regions provide a favorable condition for the development of MJI. If substructures emerge from gravitational runaway of gas inside spiral arms, their origin is presumably MJI rather than swing amplification.

Using two-dimensional numerical simulations, Kim & Ostriker (2002) have demonstrated that the MJI operating inside spiral arms is indeed much more efficient to form spiral arm substructures than swing amplification. Figure 2 shows snapshots of spurs from a model that follows the two-dimensional evolution of perturbations applied to the top of the one-dimensional equi-

librium shock profile shown in Figure 1. The left and middle panels display the snapshot of surface density in logarithmic grey scales as well as magnetic fields as solid lines, at $t = 1.27$ and 1.75 orbits, respectively. The right panel plots the distributions of Σ/Σ_0 (solid line) and v_y (dotted line) along the dotted line shown in the left frame. The size of the simulation box is $L_x = L_y/2 = \pi/10$ kpc.

Condensations begin to grow at the deep interior of the spiral arm by the action of the MJI. The embedded magnetic fields that are parallel to the spiral arm redistribute angular momentum such that the condensations continue to grow without spinning up. Small net shear keeps the radial wavenumbers of the perturbations small, so that the stabilizing effect of thermal pressure is weak. The material is collected mainly along the y-direction (parallel to the magnetic fields), as shown clearly in the the right panel of Figure 2. As the condensations move off the spiral shock, the expanding and shearing background flows shape them into first leading and then trailing configurations, eventually forming well-aligned narrow "spurs". The characteristic spacing of the spurs that form is found to be a few times the Jeans length at the density peak of the background spiral shock. When spurs grow sufficiently, they experience gravitational fragmentation, forming dense clumps in both spiral arm and interarm regions. The mass of each clump is typically $\sim 4\times10^6 M_\odot$, corresponding to the Jeans mass at the density peak. These clumps may represent giant molecular clouds or H I superclouds or, when evolved further, OB star complexes or giant H II regions observed in spiral galaxies.

So far we have discussed the formation of spiral arm substructures in two dimensions, assuming that disks are infinitesimally thin. But, the characteristic properties of the substructures including spur separation and clump mass may differ in three dimensions. A significant drawback of the thin-disk approximation is that it overestimates self-gravity at the disk midplane, so that only weak spiral potentials allow stable equilibrium spiral shock solutions in two dimensions. Weaker self-gravity in three-dimensional disks would permit stable shock profiles for stronger spiral potentials, resulting in higher arm-to-interarm density contrast and narrower arm widths than in two-dimensional, razor-thin disks. With these modified conditions, masses of clumps that form via nonlinear fragmentation of spurs in three-dimensional models might be quite different from those in two-dimensional models. Our preliminary work on the formation of spiral arm structures in a vertically extended disk shows that compared to two-dimensional models, the finite thickness of disks decreases the number of spurs by about a factor of 2 and increases the average clump mass by about a factor of 4 (Kim & Ostriker 2004, in preparation). Comparison between kinematic properties of spurs and giant clumps from these thee-dimensional simulations and high-resolution radio observations will tell if the spur forming mechanism is truly MJI.

IV. SUMMARY

One of the key unsolved problems in the structural evolution of disk galaxies is how intermediate-scale structures such as gaseous spurs, complexes of giant clouds, and giant H II regions form. Various observational evidence and theoretical arguments suggest that these intermediate-scale structures originate from gravitational instability occurring inside magnetized spiral arms. Numerical simulations show that spur structures develop as a natural consequence of the MJI for which the presence of magnetic fields and weak shear is essential to grow condensations. The shearing and expanding flow downstream from spiral shocks sculpts the shapes of spurs such that they begin to grow immediately behind the shock in the direction perpendicular to the arms and then trail away in the interarm regions. The typical separation of spurs along the arm in two-dimensional simulations is a few times the local Jeans length at the spiral arm density peak, although a smaller number of spurs is predicted to form in three dimensions. In the highly nonlinear stage, these spurs experience gravitational fragmentation to form bound condensations in both spiral arm and interarm regions. Fragments with mass each similar to the local Jeans mass at the spiral arm density peak may evolve into bright arm and interarm H II regions in spiral galaxies.

ACKNOWLEDGEMENTS

This work is a part of my Ph.D. dissertation that I conducted at the University of Maryland. I am grateful to my advisor, Eve Ostriker, for her untiring patient and stimulating advice.

REFERENCES

Baade, W. 1963, in The Evolution of Stars and Galaxies, ed. C. Payne-Gaposchkin (Cambridge: Harvard Univ. Press), 218

Blitz, L., & Shu, F. H. 1980, ApJ, 238, 148

Blitz, L., & Williams, J. P. 1999, in The Origin of Stars and Planetary Systems, eds. C. J. Lada & N. D. Kylafis (Dordrecht: Kluwer), 3

Dame, T. M., Elmegreen, B. G., Cohen, R. S., & Thaddeus, P. 1986, ApJ, 305, 892

Elmegreen, B. G., & Elmegreen, D. M. 1983, MNRAS, 203, 31

Elmegreen, B. G. 1987, ApJ, 312, 626

Elmegreen, B. G. 1995, in The 7th Guo Shoujing Summer School on Astrophysics: Molecular Clouds and Star Formation, eds. C. Yuan & Hunhan You (Singapore:World Scientific), 149

Goldreich, P., & Lynden-Bell, D. 1965, MNRAS, 130, 97

Hawley, J. F., Gammie, C. F., & Balbus, S. A. 1995, ApJ, 440, 742

Jeans, J. H. 1902, Phil. Trans. Roy. Soc. London, A199, 1

Kim, J., Franco, J., Hong, S. S., Santillán, A., & Martos, M. A. 2000, ApJ, 531, 873

Kim, W.-T., & Ostriker, E. C. 2001, ApJ, 559, 70

Kim, W.-T., & Ostriker, E. C. 2002, ApJ, 570, 132

Kim, W.-T., Ostriker, E. C., & Stone, J. M. 2002, ApJ, 581, 1080

Kim, W.-T., Ostriker, E. C., & Stone, J. M. 2003, ApJ, 599, 1157

Kim, W.-T., Hong, S. S., Yoon, S.-C., Lee, S. M., & Kim, J. 1999, in Numerical Astrophysics, eds. S. M. Miyama, K. Tomisaka, & T. Hanawa (Boston: Kluwer), 111

Klein, R. I., Woods, T., & McKee, C. F. 2001, BAAS, 33, 915

Lachièze-Rey, M., Asséo, E., Cesarsky, C. J., & Pellat, R. 1980. ApJ, 238, 175

Lattanzio, J. C., Monagahan, J. J., Pongracic, H., & Schwarz, M. P. 1985, MNRAS, 215, 125

Lin, C. C., & Shu, F. H. 1964, ApJ, 140, 646

Lin, C. C., & Shu, F. H. 1966, Proc. Nat. Acad. Sci., 55, 229

Lynden-Bell, D. 1966, Observatory, 86, 57

Mouschovias, T. Ch. 1974, ApJ, 192, 37

Oort, J. H. 1954, Bull. Astron. Inst. Netherlands, 12, 177

Parker, E. N. 1966, ApJ, 145, 811

Parker, E. N. 1967, ApJ, 149, 535

Santillán, A., Kim, J., Franco, J., Martos, M., Hong, S. S., & Ryu, D. 2000, ApJ, 545, 353

Scoville, N., & Rector, T. 2001, HST press release ; at http://oposite.stsci.edu/pubinfo/PR/2001/10/index.html

Scoville, N. Z., Polletta, M., Ewald, S., Stolovy, S. R., Thompson, R., & Rieke, M. 2001 AJ, 122, 3017

Solomon, P. M., Rivolo, A. R., Barrett, J., & Yahil, A. 1987, ApJ, 319, 730

Toomre, A. 1964, ApJ, 139, 1217

Vogel, S. N., Kulkarni, S. R., & Scoville, N. Z. 1988, Nature, 334, 402